CONDITIONAL ATTRIBUTION OF THE 2018 SUMMER EXTREME HEAT OVER NORTHEAST CHINA: ROLES OF URBANIZATION, GLOBAL WARMING, AND WARMING-INDUCED CIRCULATION CHANGES

Chunlüe Zhou, Deliang Chen, Kaicun Wang, Aiguo Dai, and Dan Qi

The probability of the record-breaking summer heat of 2018 over Northeast China was increased by a combination of human-caused climate change influences on thermodynamics and circulation, and urbanization.

The averaged near-surface air temperature (T_a) of July–August 2018 over Northeast China is ~1.73°C above the 1971–2000 mean, the highest since 1961. One-third of the stations in the region broke the historical record (Figs. 1a,b), which posed a great threat to local ecosystems and human health because this region has seldom experienced such extreme heats in previous decades (Chen et al. 2019).

In addition to influences from global warming, summer hot days over Northeast China are typically accompanied by local anticyclonic anomalies (Chen et al. 2019; Wu et al. 2011), which provide favorable conditions for increased solar radiation-induced diabatic heating due to reduced cloud cover and subsidence-induced adiabatic heating (Chen and Lu 2015; He et al. 2018). Therefore, relative contributions from atmospheric circulation anomaly and global warming to the probability of such extreme summer heats are first investigated.

More importantly, we further quantify contributions of warming-induced circulation changes to such summer heats. Global warming may induce atmospheric circulation changes, which in turn can influence the intensity and frequency of heat waves (Horton et al. 2015; Zhou et al. 2019). However, few studies have quantified this effect, likely due to weak signal of climate change compared with large natural variability in atmospheric circulation. Thanks to the acceptable performance of CMIP5-simulated circulations at monthly time scales (see Figs. ES1 and ES2 in the online supplemental material), we make such an attempt to estimate the contribution from warming-induced circulation changes to the 2018 summer heat. Besides, the urban heat island effect makes T_a over urban areas higher than that of rural regions (Zhou et al. 2019), which could intensify summer heat. The contribution from urbanization to the 2018 summer heat is also examined in this study.

Therefore, this study tries to answer three questions: 1) What does the extreme summer heat of 2018 over Northeast China look like in a historical context? 2) How much does an anticyclone contribute to the 2018 summer heat? 3) What are relative roles of urbanization, global warming, and warming-induced circulation changes in forming the 2018 summer heat?

DATA AND METHODS. Daily T_a from 1961 to 2018 at ~690 meteorological stations over Northeast China (Fig. 1a) were collected (http://data.cma.cn/). The T_a dataset has undergone quality control tests including outlier and duplicates identification, and spatial and temporal consistency checks (Zhou et al. 2018).
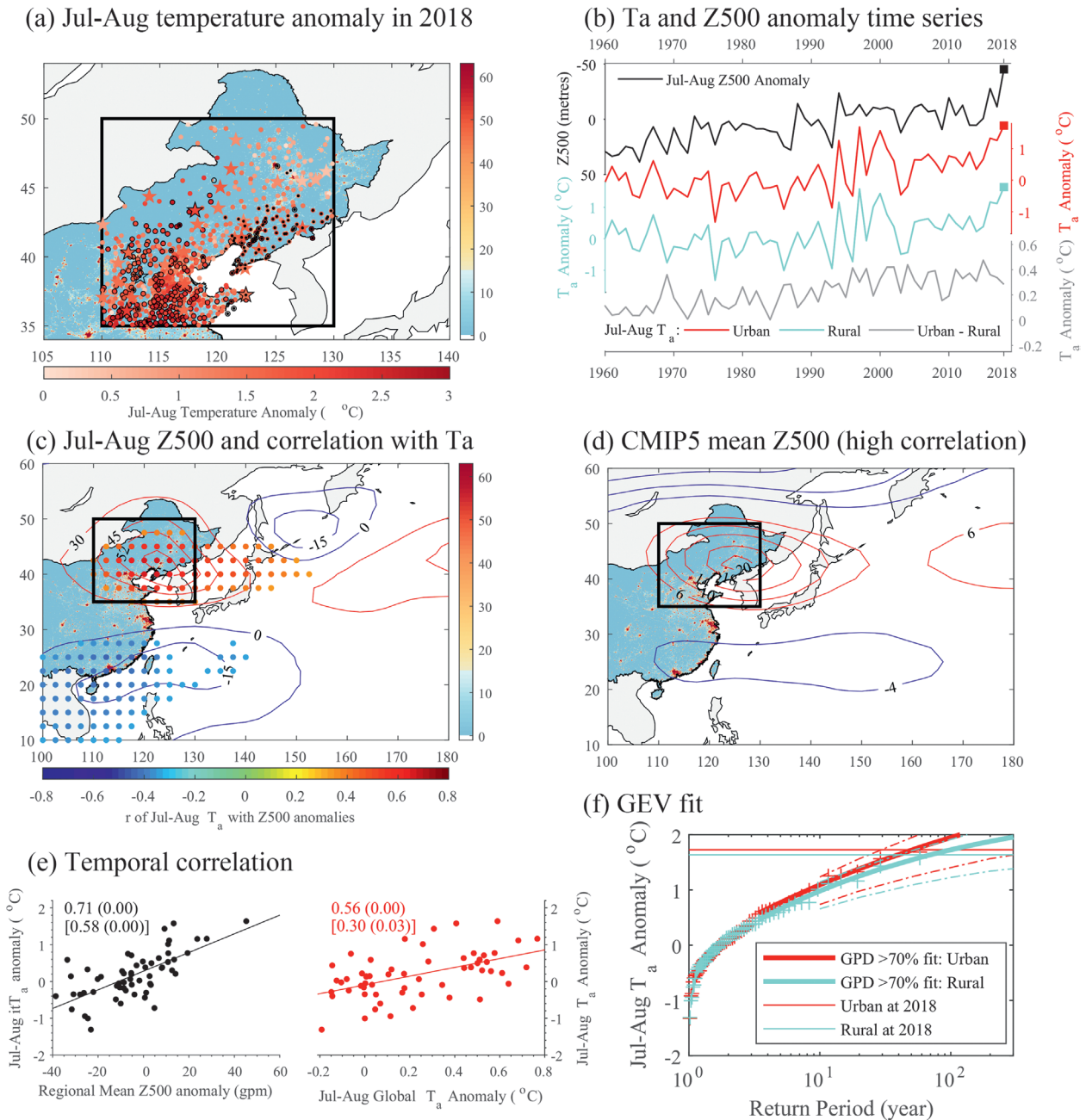
AFFILIATIONS: Zhou and Dai—Department of Atmospheric and Environmental Sciences, University at Albany, State University of New York, Albany, New York; Chen—Regional Climate Group, Department of Earth Sciences, University of Gothenburg, Gothenburg, Sweden; Wang—College of Global Change and Earth System Science, Beijing Normal University, Beijing, China; Qi—National Meteorological Center, China Meteorological Administration, Beijing, China
CORRESPONDING AUTHOR: Dr. Chunlüe Zhou, chunluezhou@gmail.com

(a) Jul-Aug temperature anomaly in 2018

(b) Ta and Z500 anomaly time series

(c) Jul-Aug Z500 and correlation with Ta

(d) CMIP5 mean Z500 (high correlation)

(e) Temporal correlation

(f) GEV fit

FIG. 1. (a) Spatial pattern of the observed July–August temperature (T_a) anomalies in 2018 over Northeast China. Stations having record-breaking July–August (daily) temperatures in 2018 summer since 1961 are marked with black edges (dots). Urban and rural stations are plotted as color-filled circles and pentagrams. (b) Time series of $Z500$ anomalies (in black) over the study region, and T_a over urban (in red), rural regions (in cyan) and their difference (in light black), relative to the period 1971–2000. Squares represents broken records in 2018. (c) Circulation regime in July–August 2018 (in red/blue contours). Correlations between the detrended region-averaged T_a and gridded $Z500$ are shown as color-filled circles ($p < 0.01$). (d) CMIP5-multi-ensemble-mean $Z500$ anomalies under high-correlation regimes from 40 ALL simulations. (e) Scatterplots of T_a with $Z500$ and global-mean T_a. Correlations were calculated before and after detrending (coefficients and significance levels in square brackets). (f) GDP fit (in solid) of T_a.

Based on Ren et al. (2015) and Zhou et al. (2019), 30 rural stations (stars in Fig. 1a) were identified in comparison with urban stations for quantifying the effect of urbanization (Sun et al. 2016). The latest stable night lights in 2013 from the Defense Meteorological Satellite Program (http://ngdc.noaa.gov/eog/

dmsp) were further used to show urban (light index >15) and rural regions (≤15). The July–August 2018 circulation anomaly regime (Fig. 1c) was depicted by the 2.5° × 2.5°500-hPa geopotential height ($Z500$) from NCEP-R1 (https://www.esrl.noaa.gov/) (Kalnay et al. 1996).

CMIP5 model outputs (http://cmip-pcmdi.llnl.gov/cmip5/) (Taylor et al. 2012) were used to quantify human influences on the probability of the 2018 summer heat. We first tested probability distributions of July–August T_a and $Z500$ anomalies from the CMIP5 historical all-forcings (ALL) simulations against observations via a Kolmogorov–Smirnov test ($p > 0.05$). Second, we assessed and selected the ALL simulations with a significant positive temporal correlation ($p < 0.05$) between the detrended July–August T_a and $Z500$ anomalies. As a result, 40 out of 54 simulations from 11 models were selected for this study, with the ALL runs extended through 2018 using the RCP4.5 runs ($58 × 40$ samples) and the corresponding natural-forcings-only runs (NAT) ending in 2012 ($52 × 40$ samples; Table ES1). Detailed time series can be seen in Fig. ES1.

To separate contributions from global warming and warming-induced circulation changes to the probability of the 2018 summer heat, following Christidis and Stott (2015), we defined years with CMIP5-based circulation regimes in individual model runs similar to the observed in July–August 2018 (i.e., a deep anticyclone within black rectangle in Fig. 1c) as high correlation years (pattern correlation ≥ 0.5; CMIP5 multimodel mean $Z500$ anomalies in Fig. 1d; more details in Fig. ES2), and defined neutral years with pattern correlations of −0.1 to 0.1. We realized that global warming in ALL runs will increase $Z500$ over most of globe including Northeast China, and such a background change in $Z500$ may not necessarily intensity the anomalous anticyclonic circulation over Northeast China, which requires further investigation. Therefore, the $Z500$ anomalies gradient was adopted to provide a better measure of the change in the circulation strength in this study.

To be consistent, observation and model data were converted into anomalies relative to the 1971–2000 mean; first regridded onto thirty 2.5° × 2.5° grids and then area-averaged over the study region (110°–130°E, 35°–50°N; Fig. 1a). Several statistical techniques were exploited:

1) Following Schaller et al. (2016), generalized Pareto distribution (GPD) with a properly selected threshold was used to fit the July–August T_a and $Z500$ anomalies.

2) The probability ratio [$PR1 = P_{(Ta\text{-}urban|urban)}/P_{(Ta\text{-}urban|rural)}$] was first calculated to quantify the urbanization effect on the likelihood of the 2018 summer heat (defined as ≥1.73°C averaged in urban regions over Northeast China). Here, $P_{(Ta\text{-}urban|urban)}$ and $P_{(Ta\text{-}urban|rural)}$ represent the probabilities of T_a anomalies exceeding 1.73°C in urban and rural scenarios.

3) After excluding the urban heat island effect, another $PR2 = P_{(Ta\text{-}rural|ALL\text{-}highZ500)}/P_{(Ta\text{-}rural|ALL\text{-}neutralZ500)}$ was calculated to estimate the role of an anticyclone existence in the probability of the 2018 summer heat. Here, $P_{(Ta\text{-}rural|ALL\text{-}highZ500)}$ and $P_{(Ta\text{-}rural|ALL\text{-}neutralZ500)}$ represent the probabilities of T_a anomalies to exceed 1.64°C (averaged in rural regions) under the high and neutral $Z500$ regimes in the ALL runs. $PR3 = P_{(Ta\text{-}rural|ALL\text{-}highZ500)}/P_{(Ta\text{-}rural|NAT\text{-}highZ500)}$] was used to quantify the influence of global warming (i.e., human-induced thermodynamical contribution). To further quantitively estimate the role of anthropogenic warming-induced circulation changes (i.e., human-induced dynamical contribution), we applied Bayesian statistics (Gelman et al. 2013; Yiou 2017) to modify PR as $PR4 = [P_{(ALL\text{-}highZ500)}/P_{(NAT\text{-}highZ500)}]·[P_{(highZ500|NAT\text{-}Ta\text{-}rural)}/P_{(highZ500|ALL\text{-}Ta\text{-}rural)}]$. Here, $P_{(Ta\text{-}rural|NAT\text{-}highZ500)}$ represents the probability of T_a anomaly to exceed 1.64°C under the high $Z500$ regime in NAT runs; and $P_{(highZ500|ALL\text{-}Ta\text{-}rural)}$ and $P_{(highZ500|NAT\text{-}Ta\text{-}rural)}$ represent the probabilities of circulation anomaly regimes similar to the 2018 observed regime when such extreme summer heats (≥1.64°C) occur in ALL and NAT runs. 95% confidence intervals (CI) were estimated with a 1000-member bootstrap (with replacement) .

RESULTS. *Role of the anticyclone.* In 2018 summer, the 5,880-m contour of the western Pacific subtropical high moved northwestward and brought the record-breaking anticyclone anomaly over Northeast China (black square in Fig. 1b) , leading to the record-breaking summer heat of 2018 over both urban and rural areas (Figs. 1a,b). New daily T_a records were registered at stations near the center of the anomalous anticyclone (black dots in Fig. 1a). Figure 1c shows strong correlations between the detrended July–August T_a and $Z500$ anomalies (associated with local anticyclones) with correlation coefficient (r) of 0.71 ($p = 0.00$) in the study region (Fig. 1e).

The likelihoods of the 2018 summer heat in high-correlation years (with the pattern shown in Fig. 1d) and neutral years in ALL runs are 11% (20 out of 224 samples) and 2% (8 out of 437 samples), respectively

(Fig. 2a). In other words, an anomalous anticyclone could increase the PR to 6 (95% CI: 4–9; Fig. 2d).

Influence of urbanization. The record-breaking July–August T_a anomalies of 2018 occurred not only in the urban areas (averaged 1.73°C; black-edged circles in Fig. 1a), but also at rural stations (averaged 1.64°C; black-edged pentagrams in Fig. 1a). A Student's *t* test of temperature differences in 2018 between the 2.5° × 2.5° urban and rural grids shows a significance level of 0.07. The metropolitan area has vast built-up surfaces and frequent human activities, leading to higher temperatures than at rural stations (Fig. 1b). A GPD fit of the observed July–August T_a anomalies suggests that the 2018 extreme summer heat is a 1-in-60-year event (95% CI: 30–500) for the urban regions and a 1-in-80-year event (95% CI: 40–10^5) for the rural regions (Fig. 1f).

Compared with the probabilities of T_a anomaly exceeding 1.73°C in urban and rural scenarios (based on PR1; Fig. 1f), urbanization increases the PR to 1.17 (95% CI: 1–10^2) (Fig. 2e); that is, ~17% increase in the likelihood.

Influences of global warming and warming-induced circulation changes. July–August T_a anomalies over Northeast China significantly correlate with July–August global-mean temperature ($r = 0.56$, $p = 0.00$) (Fig. 1e), implying a strong footprint of global warming on the 2018 summer heat over Northeast China.

Compared with the probabilities of T_a anomaly exceeding 1.64°C under similar circulation regimes in ALL and NAT runs (based on PR3; Fig. 2a), we found that global warming has increases the probability by ~78% (95% CI: 53%–128%; Fig. 2f).

Global warming has been argued to have caused atmospheric circulation changes that have altered regional extreme events in different ways (Horton et al. 2015; Schär et al. 2004; Zhou and Wang 2016), increasing attribution challenge of human-induced dynamical and thermodynamical contributions to odds of the event.

The probabilities of CMIP5-simulated circulation regimes similar to the 2018 observed regime over Northeast China (i.e., with pattern correlations being 0.5 or more) are almost equivalent in ALL and NAT runs (Fig. 2b), but the intensity of the circula-
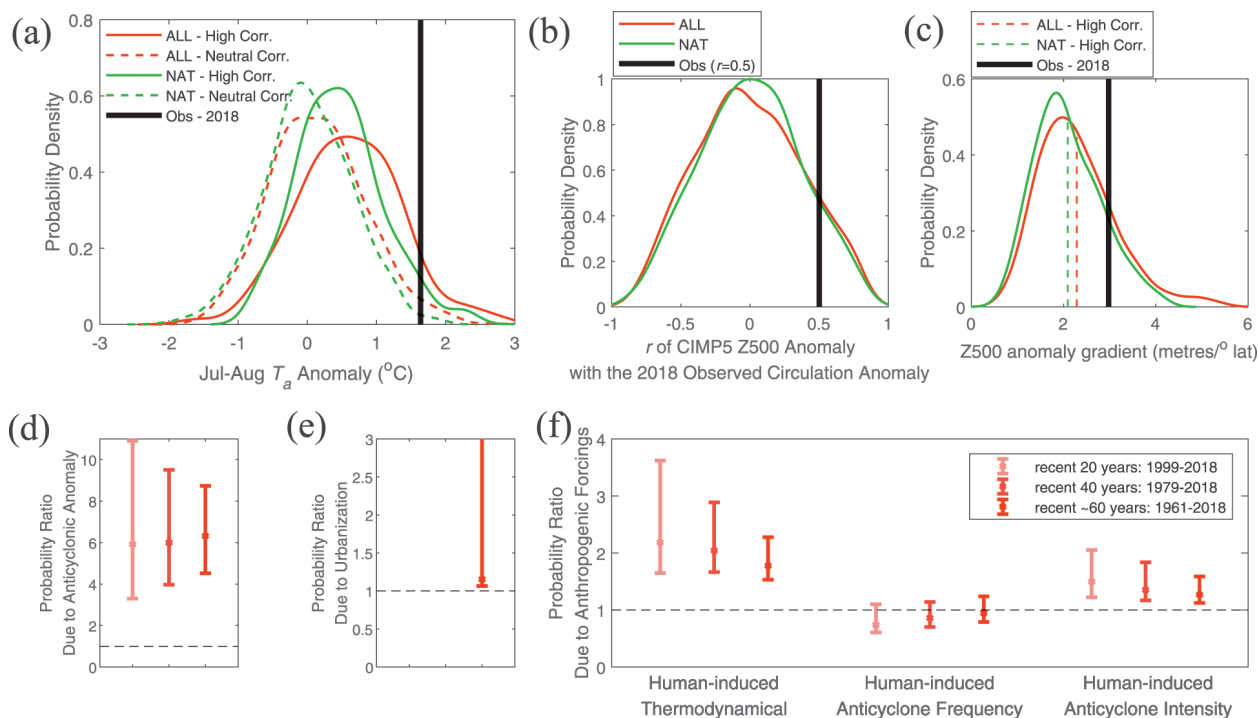
FIG. 2. (a) Probability density of July–August temperature anomalies (T_a) under high (in solid) and neutral (in dash) regimes in 40 all-forcings (ALL; in red) and natural-forcing-only (NAT; in green) simulations. The thick black line is the observed T_a of July–August 2018 over rural regions. (b) Probability density of pattern correlation coefficients (*r*) between CMIP5-based $Z500$ regimes and the 2018 observed regime in ALL/NAT runs. (c) Probability density of $Z500$ anomaly gradients with *r* > 0.5. Dashed lines are their mean. (d) Probability ratio (PR) of the 2018 summer heat due to the occurrence of anticyclone. (e) PR due to urbanization. (f) PR due to human influences from human-induced dynamical (frequency and intensity) and thermodynamical changes.

tion anomalies in high-correlation years increases by ~11% in ALL runs relative to NAT runs (mean of 2.29 vs 2.07 m per degree of latitude described by the $Z500$ anomaly gradient in Fig. 2c). These results imply that global warming has altered the $Z500$ field by strengthening the anomalous anticyclone over Northeast China, which in turn may have enhanced the severity of the 2018 summer heat.

Compared with the probabilities of T_a anomaly exceeding 1.64°C and circulation regimes similar to the 2018 observed regime in ALL and NAT runs (based on PR4), we found that an increased likelihood by ~27% (95% CI: 12%–59%) is attributable to the warming-induced circulation intensity change over Northeast China, while the warming-induced circulation frequency change has no significant impact on the likelihood (Fig. 2f).

CONCLUSIONS AND DISCUSSION. Our analyses based on surface observations and reanalysis fields indicate the record-breaking temperature and circulation anomalies in 2018 summer over Northeast China. Return period of the 2018 summer heat is 1-in-60 years for the urban areas and 1-in-80 years for the rural areas. CMIP5-based analyses suggest that the existence of an anomalous anticyclone over Northeast China increases the odds of the 2018 summer heat to 6.16 times that without such an anticyclone.

Based on the GPD fits, we found that urbanization over the metropolitan areas might have increased the likelihood of the 2018 summer heat by ~17%. After excluding the urbanization effect, CMIP5-based PR analyses suggest that anthropogenic global warming may have increased the probability of the 2018 summer heat over Northeast China by ~78%. Global warming has strengthened the anticyclonic circulation by ~11%, which may have increased the likelihood (by ~27%) of the 2018 summer heat over Northeast China.

In summary, an anomalous anticyclonic circulation over Northeast China was the main cause of the 2018 summer heat. Global warming and warming-induced circulation intensity change have increased the odds, and urbanization has further exacerbated the 2018 summer heat over Northeast China.

The non-stationary of the time series would consistently increase the attribution uncertainties for all the factors (Figs. 2d,e), but it does not change our main conclusions.

REFERENCES

Chen, R., and R. Lu, 2015: Comparisons of the circulation anomalies associated with extreme heat in different regions of eastern China. *J. Climate*, **28**, 5830–5844, https://doi.org/10.1175/JCLI-D-14-00818.1.

——, Z. Wen, and R. Lu, 2019: Influences of tropical circulation and sea surface temperature anomalies on extreme heat over Northeast Asia in the midsummer of 2018. *Atmos. Oceanic Sci. Lett.*, **12**, 238–245, https://doi.org/10.1080/16742834.2019.1611170.

Christidis, N., and P. A. Stott, 2015: Extreme rainfall in the United Kingdom during winter 2013/14: The role of atmospheric circulation and climate change [in "Explaining Extreme Events of 2014 from a Climate Perspective"]. *Bull. Amer. Meteor. Soc.*, **96** (12), 46–50, https://doi.org/10.1175/BAMS-D-15-00094.1.

Gelman, A., H. S. Stern, J. B. Carlin, D. B. Dunson, A. Vehtari, and D. B. Rubin, 2013: *Bayesian Data Analysis*. 3rd ed. Chapman and Hall/CRC, 675 pp.

He, Y., K. Wang, C. Zhou, and M. Wild, 2018: A revisit of global dimming and brightening based on sunshine duration. *Geophys. Res. Lett.*, **45**, 4281–4289, https://doi.org/10.1029/2018GL077424.

Horton, D. E., N. C. Johnson, D. Singh, D. L. Swain, B. Rajaratnam, and N. S. Diffenbaugh, 2015: Contribution of changes in atmospheric circulation patterns to extreme temperature trends. *Nature*, **522**, 465–469, https://doi.org/10.1038/nature14550.

Kalnay, E., and Coauthors, 1996: The NCEP/NCAR 40-Year Reanalysis Project. *Bull. Amer. Meteor. Soc.*, **77**, 437–471, https://doi.org/10.1175/1520-0477(1996)077<0437:TNYRP>2.0.CO;2.

Ren, G., and Coauthors, 2015: An integrated procedure to determine a reference station network for evaluating and adjusting urban bias in surface air temperature data. *J. Appl. Meteor. Climatol.*, **54**, 1248–1266, https://doi.org/10.1175/JAMC-D-14-0295.1.

Schaller, N., and Coauthors, 2016: Human influence on climate in the 2014 southern England winter floods and their impacts. *Nat. Climate Change*, **6**, 627–634, https://doi.org/10.1038/nclimate2927.

Schär, C., P. L. Vidale, D. Lüthi, C. Frei, C. Häberli, M. A. Liniger, and C. Appenzeller, 2004: The role of increasing temperature variability in European summer heatwaves. *Nature*, **427**, 332–336, https://doi.org/10.1038/nature02300.

Sun, Y., X. Zhang, G. Ren, F. W. Zwiers, and T. Hu, 2016: Contribution of urbanization to warming in China. *Nat. Climate Change*, **6**, 706–709, https://doi.org/10.1038/nclimate2956.

Taylor, K. E., R. J. Stouffer, and G. A. Meehl, 2012: An overview of CMIP5 and the experiment design. *Bull. Amer. Meteor. Soc.*, **93**, 485–498, https://doi.org/10.1175/BAMS-D-11-00094.1.

Wu, R., S. Yang, S. Liu, L. Sun, Y. Lian, and Z. Gao, 2011: Northeast China summer temperature and North Atlantic SST. *J. Geophys. Res.*, **116**, D16116, https://doi.org/10.1029/2011JD015779.

Yiou, P., 2017: A statistical framework for conditional extreme event attribution. *Adv. Stat. Climataol. Meteor. Oceanogr.*, **3**, 17–31, https://doi.org/10.5194/ascmo-3-17-2017.

Zhou, C., and K. Wang, 2016: Coldest temperature extreme monotonically increased and hottest extreme oscillated over Northern Hemisphere land during last 114 years. *Sci. Rep.*, **6**, 25721, https://doi.org/10.1038/srep25721.

——, Y. He, and K. Wang, 2018: On the suitability of current atmospheric reanalyses for regional warming studies over China. *Atmos. Chem. Phys.*, **18**, 8113–8136, https://doi.org/10.5194/acp-18-8113-2018.

——, K. Wang, D. Qi, and J. Tan, 2019: Attribution of a record-breaking heatwave event in summer 2017 over Yangtze River Delta [in "Explaining Extreme Events of 2017 from a Climate Perspective"].*Bull. Amer. Meteor. Soc.*, **100** (1), S97–S103, https://doi.org/10.1175/BAMS-D-18-0134.1.